

HyPE-GT: where Graph Transformers meet Hyperbolic Positional Encodings

Kushal Bose and Swagatam Das

Abstract

Graph Transformers (GTs) facilitate the comprehension of graph-structured data by calculating the self-attention of node pairs without considering node position information. To address this limitation, we introduce an innovative and efficient framework that introduces Positional Encodings (PEs) into the Transformer, generating a set of learnable positional encodings in the hyperbolic space, a non-Euclidean domain. This approach empowers us to explore diverse options for optimal selection of PEs for specific downstream tasks, leveraging hyperbolic neural networks or hyperbolic graph convolutional networks. Additionally, we repurpose these positional encodings to mitigate the impact of over-smoothing in deep Graph Neural Networks (GNNs). Comprehensive experiments on molecular benchmark datasets, co-author, and co-purchase networks substantiate the effectiveness of hyperbolic positional encodings in enhancing the performance of deep GNNs.

Index Terms

Graph Transformers, Attention, Hyperbolic Spaces, Convolution, Positional Encoding.



1 INTRODUCTION

GRAPH Transformers (GTs) are earmarked as one of the milestones for modelling the interactions between the node pairs in the graph. As the existing graph neural network suffers from a few glaring shortcomings like over-smoothing [1] which occurs due to the recursive neighborhood aggregation, over-squashing [2], an information bottleneck caused by the exponential growth of information while increasing the size of the receptive field, and bounded expressive power [3], [4]. Graph Transformers confront the limitations by evaluating pair-wise self-attention without considering the structural inductive bias which causes the loss of positional information of the nodes. As an effective solution, the positional encodings as vectors are integrated with the node features to make the respective nodes topologically aware in the graph. Recently, many efforts were made to generate effective positional encodings for the GTs like spectral decomposition-based learnable encoding [5], structure-aware PEs generated from the rooted subgraph or subtree of the nodes [6], encoding the structural dependency [7], random walk-based learnable positional encodings [8] and many more.

The positional encodings derived from existing works suffer from several key limitations like Spectral Attention Network (SAN) which generates learnable positional encodings by spectral decomposition of the Laplacian matrix. SAN requires high computational time as well as memory, especially for the generation of edge-feature-based Laplacian positional encodings. Structure-aware Transformers (SAT) estimates pairwise attention scores depending on the respective rooted sub-graphs or sub-trees. SAT requires to extract multi-hop subgraphs resulting in an increase in the pre-processing time and consumption of high memory. To alleviate the shortcomings, we propose a novel framework named **Hyperbolic Positional Encodings based Graph Transformer** or **HyPE-GT** which is capable to generate a set of learnable positional encodings in the hyperbolic space. To the best of our knowledge, we are the first to foster hyperbolic geometry in designing positional encodings for the Graph Transformers.

HyPE-GT introduces learnable hyperbolic positional encodings, depending on three key modules: the initialization of PEs (PE_{init}), the manifold type (M), and the hyperbolic network type (HN), transforming the PEs into the hyperbolic space. Each module comprises multiple entities, and each positional encoding results from selecting a unique triplet from one entity of each module. The maximum number of positional encodings is given by $|PE_{init}| \times |M| \times |HN|$, with the framework offering diverse design choices based on entity selection, generating varied PEs. These hyperbolic positional encodings provide practitioners with versatile options for optimizing downstream tasks. The learnable hyperbolic PEs seamlessly integrate with standard graph transformers, supplying essential positional information. Additionally, we leverage positional encodings to enhance deep Graph Neural Networks (GNNs) by mitigating over-smoothing, incorporating hyperbolic PEs with Euclidean node features from hidden layers in deep GNN architectures.

Contribution Our contributions throughout the paper can be summarized in the following way: (1) We propose a novel and powerful framework named as HyPE-GT which generates a set of learnable positional encodings in the hyperbolic space, a non-euclidean domain. We are the first to incorporate hyperbolic PEs with the Euclidean Graph Transformer. The PEs are learned by passing through either hyperbolic neural networks or hyperbolic graph convolutional networks which produces a useful positional encodings and structural encodings. (2) We propose two different strategies to combine

• *Electronics and Communication Sciences Unit, Indian Statistical Institute, Kolkata, India.*

E-mail: kushalbose92@gmail.com, swagatam.das@isical.ac.in

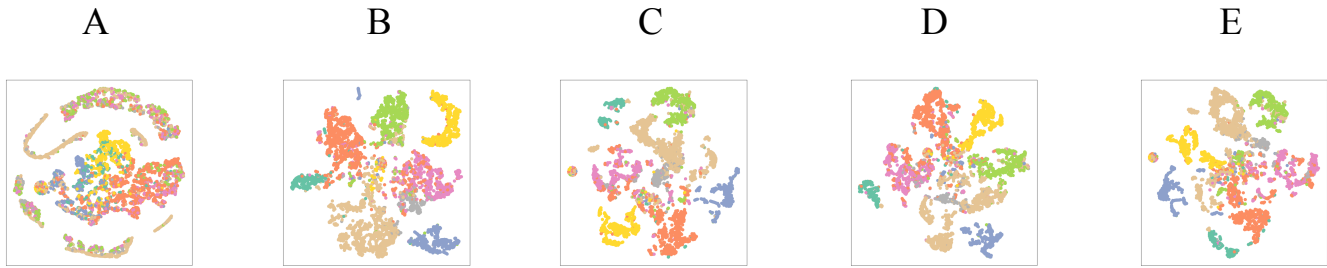


Fig. 1: The visualization of node embeddings of Amazon Photo dataset generated by 128-layered GCN for the PE category of 4. A. Node embeddings without using any positional encodings. B. Node embeddings with using HyPE framework. C. Embeddings of hyperbolic PEs from HyPE. D. Node embeddings with using HyPEv2 framework. E. Embeddings of hyperbolic PEs from HyPEv2.

hyperbolic PEs with the Euclidean node features which resulting in two different variants as **HyPE-GT** and **HyPE-GTv2**. (3) The hyperbolic positional encodings are re-purposed to diminish the effect of over-smoothing in deep GNN models.

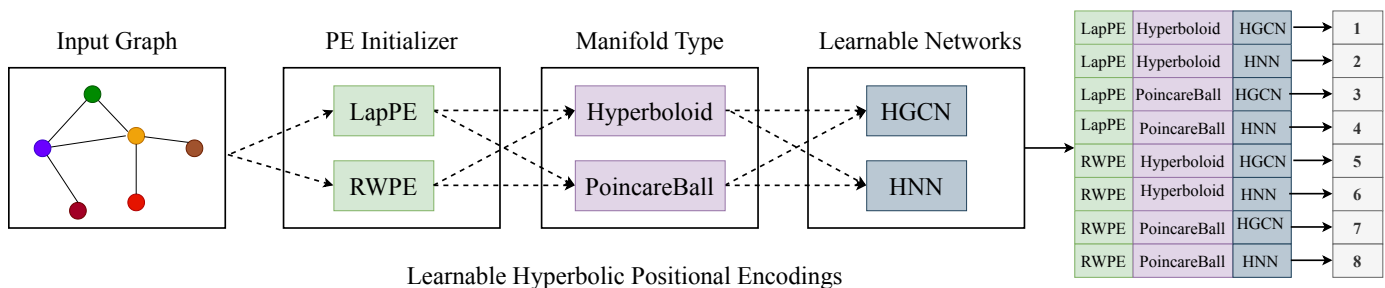


Fig. 2: Schematic representation of the process for generating a family of learnable hyperbolic positional encodings (8 different categories) in the HyPE-GT framework. Each category can be generated by following a particular path (shown with arrow-marked dotted lines) which begins from PE initialization block and ends to the learnable hyperbolic networks block. Each positional encoding is assigned with a unique number shown in the right side of the diagram.

2 RELATED WORKS

Graph Transformers The attention mechanism on the graph data is primarily introduced with Graph Attention Network (GAT) [9]. But GAT is only capable of learning from the connected neighborhoods via sparse message passing. The limitation is overcome when Dwivedi and Bresson generalized the Transformer architecture for the graphs [10] and showed its utility on various categories of tasks. Later many other significant approaches were made like Spectral Attention Network (SAN) [5] which relies on learning the eigenvectors of the Laplacian matrix. The learnable eigenvectors act as PE, which is concatenated with the original node features for the Transformer. Structure-aware Transformer (SAT) [6] computes the self-attention among node pairs by incorporating structural information of the extracted subgraphs rooted at each node. Another line of work GraphiT [11] learns relative positional encoding via diffusion kernels which computes attention between the node pairs. On the other hand, Graphormer [7] designs spatial representations like degree encoding, edge encoding, etc. which capture the structural dependency of the graph. The encodings are added as the bias terms in the self-attention matrix. GraphTrans [12] proposes a model which first learns from multiple GNN layers stacked together and then the updated node representations are provided as input to the standard Graph Transformer layer. Recently, another framework GraphGPS [13] allows module-wise selection like message-passing module and global attention module which helps to design efficient Graph Transformers. TokenGT [14] considers every node and edge of the graph as independent tokens. The tokens are associated with token embeddings which are the input to the standard Transformer. Edge-augmented Graph Transformer (EGT) [15] introduces edge embeddings for every pair of nodes which acts as the edge gates to control information flow in the Transformer. Graph Transformer Networks (GTN) [16] and Heterogeneous Graph Transformer (HGT) [17] are dedicated to heterogeneous graphs, which extract effective meta-paths based on attention.

Hyperbolic Graph Neural Networks Recent efforts were made to make deep neural networks suitable in the non-Euclidean space like hyperbolic space equipped with negative curvature [18], [19]. Later the hyperbolic neural networks are extended for the graph-structured data as Hyperbolic Graph Neural Networks [20]. On advancement, the hyperbolic graph convolutional networks [21] and hyperbolic graph attention networks [22] strengthen the family of the hyperbolic graph neural networks.

3 PROPOSED METHOD

3.1 Preliminaries and Notations

Assume an attributed graph $\mathcal{G} = (\mathcal{V}, \mathcal{E}, X)$ where \mathcal{V} denotes a set of vertices, $\mathcal{E} \subseteq \mathcal{V} \times \mathcal{V}$ denotes set of edges, and $X \in \mathbb{R}^{n \times d}$ presents the node attributes where n denotes the number of vertices and each node is associated with a d -dimensional feature. The adjacency matrix A is the symmetric matrix with binary elements denotes the edges or node connections in the graph. D is a diagonal matrix where each element in the diagonal is the degree of the corresponding nodes.

3.2 Transformers on Graphs

Inspired from Vaswani *et al.* [23], Dwivedi, and Bresson [10] extended the philosophy of Transformer for the graph-structured data. Message Passing Graph Neural Networks (MP-GNNs) implement sparse message passing where GTs assume the fully-connected graph structure. Unlike MP-GNNs, Graph Transformers are designed to compute attention coefficient between the pairs of nodes without considering the graph structure. A single Transformer layer consists of a self-attention module which is followed by a feed-forward network. The feature matrix X is transformed into query Q , key K , and values V by multiplying with the projection matrices as $Q = XW_Q$, $K = XW_K$, and $V = XW_V$. The self-attention matrix is computed as follows,

$$X_A = \text{softmax}\left(\frac{QK^T}{\sqrt{d_{out}}}\right)V, \quad (1)$$

where $X_A \in \mathbb{R}^{n \times d_{out}}$ is the self-attention matrix with d_{out} is the output dimension. W_Q , W_K , and W_V are trainable parameters. To boost the impact of the self-attention module sometimes we employ multi-head attention (MHA) strategy. The multi-head attention is the result of the concatenation of multiple instances of the equation 1. The multi-head attention can be expressed as

$$X_A = M \parallel_{k=1}^H \left(\sum_{j \in N(i)} \alpha_{ij}^{(k)} V^{(k)} X_j \right), \quad (2)$$

where $\alpha_{ij}^{(k)}$ is the attention coefficient between node i and j from k^{th} head. M and $V^{(k)}$ are the trainable parameters and X_j is the j^{th} node features. The estimated self-attention matrix is followed by a residual connection and then passes through a feed-forward network (FFN) with the normalization layers as follows,

$$\begin{aligned} X' &= \text{Norm}(X + X_A), \\ X'' &= W_2(\text{ReLU}(W_1 X')), \\ X_o &= \text{Norm}(X' + X''), \end{aligned} \quad (3)$$

where X_o is the final output of the transformer layer and $W_1 \in \mathbb{R}^{d_{out} \times d}$, $W_2 \in \mathbb{R}^{d \times d}$ are trainable parameters. We can either use Batchnorm [24] or Layernorm [25] for the feature normalization. Each Transformer layer generates node-level representations which are permutation equivariant. The absence of positional information on the nodes generates similar outputs. Therefore, it is necessary to incorporate appropriate positional encodings to leverage the learning process in the Transformer.

3.3 Preliminaries on Hyperbolic Spaces

Hyperbolic geometry deals with the smooth manifold with constant negative curvature. Let us consider the manifold $\mathcal{M} \in \mathbb{R}^d$ embedded in \mathbb{R}^{d+1} . Let us have the following definitions.

Tangent space, Logarithmic map and Exponential map For every point $x \in \mathcal{M}$, the tangent space $\mathcal{T}_x \mathcal{M}$ is defined as a d -dimensional hyperplane approximates the \mathcal{M} around x . For any point x , we can define exponential map \exp_x as $\exp_x : \mathcal{T}_x \mathcal{M} \rightarrow \mathcal{M}$ transforms any vector in $\mathcal{T}_x \mathcal{M}$ on the \mathcal{M} . The logarithmic map \log_x is the inverse of the exponential map, that is, $\log_x : \mathcal{M} \rightarrow \mathcal{T}_x \mathcal{M}$. The Riemannian metric $g^{\mathcal{M}}$ on the manifold is defined as the inner product on the tangent space like $g^{\mathcal{M}}(\cdot, \cdot) : \mathcal{T}_x \mathcal{M} \times \mathcal{T}_x \mathcal{M} \rightarrow \mathbb{R}$. Along with these definitions we will discuss two well-adopted models from the hyperbolic geometry as following:

Hyperboloid Model One of the models in the hyperbolic geometry and also commonly known as the Lorentz model. The model is defined as Riemannian manifold $(\mathbb{H}_c^n, g_x^{\mathbb{H}})$ with negative curvature where

$$\mathbb{H}_c^n = \{x \in \mathbb{R}^{n+1} : \langle x, x \rangle_{\mathbb{H}} = -c, x_0 > 0\} \quad (4)$$

$$g_x^{\mathbb{H}} = \text{diag}([-1, 1, \dots, 1])_n, \quad (5)$$

where $\langle \cdot, \cdot \rangle$ denotes Minkowski inner product.

Poincare Ball Model Another important model is the Poincare Ball model, which is equipped with negative curvature $c(c < 0)$, is a Riemannian manifold $(\mathcal{B}_c^n, g_x^{\mathcal{B}})$ with

$$\begin{aligned} \mathcal{B}_c^n &= \{x \in \mathbb{R}^n : \|x\|^2 < -\frac{1}{c}\}, \\ g_x^{\mathcal{B}} &= \frac{2}{(1 + c\|x\|_2^2)} g^E, \end{aligned} \quad (6)$$

where g^E is the Euclidean metric which is I_n . The model represents an open ball of radius of $\frac{1}{\sqrt{c}}$.

3.4 Learnable Hyperbolic Positional Encodings: An overview

In this section, we present a brief overview of the HyPE-GT framework for the easy apprehension of the rest of the work. HyPE-GT consists of three key modules namely, (1) the initialization of the positional encodings, (2) the type of the manifolds where the transformed PEs will be projected, and the last one is (3) learning the hyperbolic positional encodings by employing either Hyperbolic Neural Network (HNN) or Hyperbolic Graph Convolutional Network (HGNCN). As we previously mentioned that the characteristics of the generated positional encodings are nothing but the manifestation of the choice of entities in those three modules. In this work, we consider two entities for each of the module like LapPE and RWPE for PE initialization, Hyperboloid and PoincareBall for manifold type, and for learnable networks we select HNN and HGNCN. Refer Figure 2 for more intricate details of the flow of the framework. So, there will be 8 different categories of PEs can be generated and each of them is assigned with a unique number from 1 – 8 for ease of reference. The rest of the paper is organized as follows to provide more insights regarding the proposed framework followed by extensive experimentation.

3.5 Initialization of Positional Encodings

The effectiveness of the learnable hyperbolic positional encodings directly depends on the initialization of positional encodings. Besides many other existing PEs [11], [26], [27], [7] etc., we adopt two well-known PE initialization techniques as proposed in [8] which are Laplacian Positional Encodings (LapPE) and Random Walk Positional Encoding (RWPE). LapPE is generated by performing eigen-decomposition of the Laplacian matrix of the input graph. For the i^{th} node, the LapPE can be presented as:

$$p_i^{\text{LapPE}} = [U_{i1}, U_{i2}, \dots, U_{ik}] \in \mathbb{R}^k, \quad (7)$$

where U_i denotes the i^{th} eigenvectors of the graph Laplacian and k elements are chosen. The i^{th} eigenvector is designated as the initialized position vector for the i^{th} node in the graph. The eigenvectors are assumed to have information of the spectral properties of the graph. The second one is the k -dimensional RWPE which is generated by k -steps of the diffusion process with the degree-normalized random walk matrix. For the i^{th} node, RWPE can be represented as follows:

$$p_i^{\text{RWPE}} = [\hat{A}_{ii}^1, \hat{A}_{ii}^2, \dots, \hat{A}_{ii}^k] \in \mathbb{R}^k, \quad (8)$$

where $\hat{A} = AD^{-1}$. RWPE captures the structural patterns of the k -hop neighborhoods. Finally, the initialization of PE module have two positional encodings.

3.6 Choice of Manifold

The whole mechanism of generating the positional encodings heavily relies on the nature of the manifolds where the initialized positional encodings will be projected. Hence, the choice of a manifold will be one of the key decisive factor for generating effective PEs as well as the performance enhancement of the Graph Transformers. In HyPE-GT, we will involve two dominant choices named `Hyperboloid` and `PoincareBall` manifolds to serve the purpose.

3.7 Learning through Hyperbolic Neural Architectures

The initialized positional encodings are learned by applying hyperbolic neural network architectures viz Hyperbolic Neural Networks and Hyperbolic Graph Convolutional Networks. let the initialized positional encodings p^{init} is transformed to $\hat{p} = W_0 p^{\text{init}}$ into some low dimensional space via the parameterized transformation W_0 . Then the \hat{p} is learnable in the following ways:

Hyperbolic Neural Network (HNN) The transformed initial positional encodings are fed into a hyperbolic multi-layered feed-forward neural network. The HNN produces encodings into the hyperbolic space by the layer-wise propagation. The transformation can be formulated as follows,

$$p^{\text{HNN}} = \text{HNN}_{\mathcal{M}}^{(L)}(\hat{p} | \Theta), \quad (9)$$

where Θ is the trainable parameters of the HNN, L denotes the number of hidden layers, and \mathcal{M} denotes the pre-defined manifold type where the learned positional encodings are projected which can be either Hyperboloid or PoincareBall. HNNs are not able to learn the structure-aware embeddings from the input graph. This limitation can be alleviated by using a graph convolutional-based architecture.

Hyperbolic Graph Convolutional Network (HGNCN) We fed the positional encodings to the hyperbolic graph convolutional networks to extract necessary information from the graph structure. Like the previous one, firstly the initial positional features are mapped into low-dimensional space and then positional encodings are learned by the hyperbolic graph convolutional network. The following equation describes the expected transformation as

$$p^{\text{HGNCN}} = \text{HGNCN}_{\mathcal{M}}^{(L)}(\hat{p} | \Phi), \quad (10)$$

where Φ denotes the trainable parameters of the HGNCN, L is the number of stacked convolutional layers, and \mathcal{M} can be either Hyperboloid or PoincareBall model. Note that, we obtain the learned positional encodings in the hyperbolic space. The learned PE will be integrated with the Transformer architecture to provide positional information of the nodes.

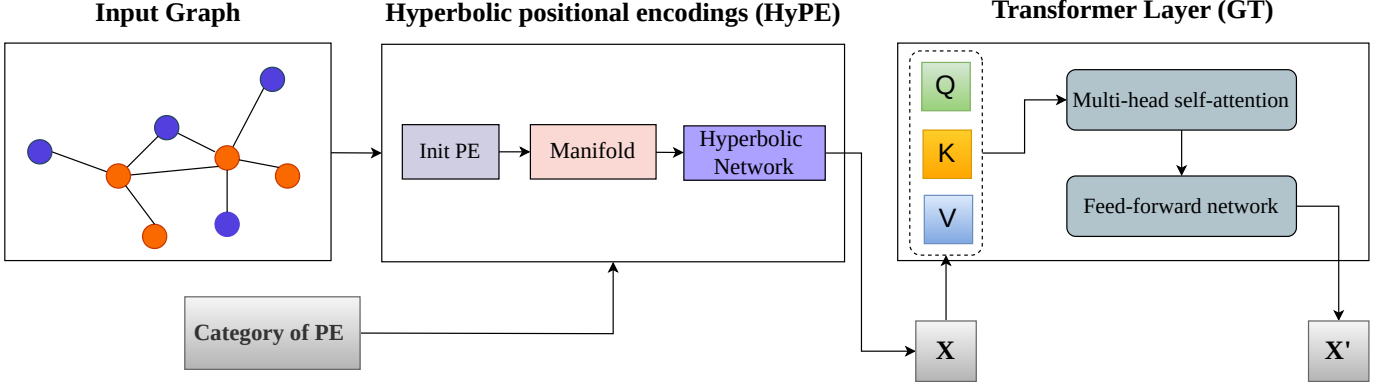


Fig. 3: The workflow of HyPE-GT is presented. The framework is the combination of two independent blocks namely hyperbolic positional encodings or HyPE and standard Graph Transformer or GT. Depending on one’s choice, HyPE will generate a fixed type of PE. The PE is added with the feature matrix X before fetching it to the Transformer layer.

TABLE 1: Performance on three benchmark datasets [28]. For each category of PE, the results are presented with mean and standard deviations from 10 runs with different random seeds. The category of PE and the optimal number of layers are mentioned respectively inside the parenthesis. The top three results **first**, **second**, and **third** are marked.

Method	PATTERN	CLUSTER	MNIST	CIFAR10
	Accuracy \uparrow	Accuracy \uparrow	Accuracy \uparrow	Accuracy \uparrow
GCN [29]	71.892 \pm 0.334	68.498 \pm 0.976	90.705 \pm 0.218	55.710 \pm 0.381
GIN [3]	85.387 \pm 0.136	64.716 \pm 1.553	96.485 \pm 0.252	55.255 \pm 1.527
GAT [9]	78.271 \pm 0.186	70.587 \pm 0.447	95.535 \pm 0.205	64.223 \pm 0.455
Gated-GCN [30]	85.568 \pm 0.088	73.840 \pm 0.326	97.340 \pm 0.143	67.312 \pm 0.311
PNA [31]	–	–	97.94 \pm 0.12	70.35 \pm 0.63
DGN [26]	86.680 \pm 0.034	–	–	72.838 \pm 0.417
GraphTransformer [10]	84.808 \pm 0.068	73.169 \pm 0.622	–	–
Graphormer [7]	–	–	–	–
k-subgraph SAT [6]	86.848 \pm 0.037	77.856 \pm 0.104	–	–
SAN [5]	86.581 \pm 0.037	76.691 \pm 0.65	–	–
EGT [15]	86.821 \pm 0.020	79.232 \pm 0.348	98.173 \pm 0.087	68.702 \pm 0.409
GraphGPS [13]	86.685 \pm 0.059	78.016 \pm 0.180	98.051 \pm 0.126	72.298 \pm 0.356
HyPE-GT (ours)	86.7794 \pm 0.0382(1, 1)	77.9275 \pm 0.1261(1, 1)	98.21 \pm 0.0007(8, 2)	70.68 \pm 0.0081(7, 2)
HyPE-GTv2 (ours)	84.9350 \pm 0.0093(3, 1)	72.8499 \pm 0.0879(1, 1)	98.18 \pm 0.0634(2, 2)	67.61 \pm 0.0087(2, 2)

3.8 Complete Pipeline of HyPE-GT framework

HyPE-GT comprises of two key modules named as HyPE which generates learnable hyperbolic positional encodings and second one is the standard Graph Transformer (GT). The HyPE is designed to produce various categories of positional encodings for a single downstream task. The category of PE is decided by choosing the three parameters namely (1) initialization of positional encodings, (2) type of the manifold, and (3) the hyperbolic networks. Figure 3 illustrates the complete workflow of the generation of hyperbolic positional encodings of a given input graph and the integration with the Transformer architecture. For an external input for the category number, we have a pre-defined triplet that produces a fixed category of positional encodings as marked from $\{1 - 8\}$. For example, if someone wants to generate the category 4 hyperbolic positional encodings, then the triplet should be like $\{\text{LapPE}, \text{PoincareBall}, \text{HGNC}\}$. In this way, HyPE-GT can produce diversified 8 different categories of positional encodings. As the generated positional encodings lie in the hyperbolic space and node features belong to the Euclidean domain. Therefore, integration of two can be implemented in a straightforward way. We devised two different strategies for addition of hyperbolic PEs with the node features as following:

Strategy 1 As the generated PEs lie in the hyperbolic space, the direct Euclidean addition with the Euclidean node features is not supported. As a solution, firstly the node features are transformed into hyperbolic space and thereafter the hyperbolic PEs are added by Möbius addition [18] which produces meaningful output. The updated node features are reverted back into the Euclidean space to provide input to the Transformer. If $p_k^{\mathbb{H}}$ is the generated positional encodings in the hyperbolic space with manifold type \mathbb{H} for the k^{th} category and $\hat{x}_v^{\mathbb{E}}$ is the initial node feature in Euclidean space for the v^{th} node, then update rule will be as following:

$$\begin{aligned}
 \hat{x}_v^{\mathbb{H}} &= \exp_o(\tan_{\text{proj}}(\hat{x}_v^{\mathbb{E}})) \\
 x_v^{\mathbb{H}} &= \hat{x}_v^{\mathbb{H}} \oplus_c p_k^{\mathbb{H}} \\
 x_v^{\mathbb{E}} &= \log_o(x_v^{\mathbb{H}}),
 \end{aligned} \tag{11}$$

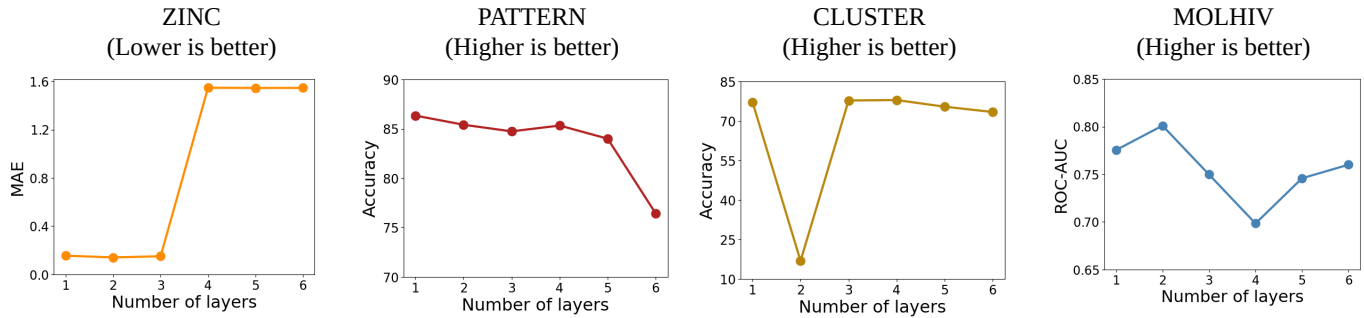


Fig. 4: Effect of depth of hyperbolic neural architectures for all five datasets. The number of layers is varied from 1 – 5. For each layer, we averaged out the values of 4 runs on different random seeds.

where $\hat{x}_v^{\mathbb{H}}$ and $x_v^{\mathbb{H}}$ are the node features in hyperbolic space before and after addition of the hyperbolic positional encodings respectively, \oplus_c denotes the Möbius addition with space curvature c . The function \tan_{proj} maps the features from Euclidean domain to the tangent space of the hyperbolic space at the point o of the manifold.

Strategy 2 In this case, firstly the hyperbolic PEs are transformed into Euclidean space and added with the Euclidean node features. We termed this variant as HyPE-GTv2. The following equations describe the rule of this variant:

$$\begin{aligned} p_k^{\mathbb{E}} &= \log_o(p_k^{\mathbb{H}}), \\ x_v^{\mathbb{E}} &= \hat{x}_v^{\mathbb{E}} + p_k^{\mathbb{E}}. \end{aligned} \quad (12)$$

The notations used carry the similar meanings as described earlier. Note that, in this case we apply Euclidean addition to combine PE and node features as both belong to the Euclidean space.

Utility in Deep GNN Models. Over-smoothing [1] is posed as a dominant challenge of the deep graph neural networks. The node features become indistinguishable due to the recursive neighborhood aggregation during the message propagation in deeper layers. Hence, we re-purpose the hyperbolic positional encodings to couple with the intermediate node features to mitigate the issue. The following equation represents the usage of positional encodings in the output of multi-layered GNNs:

$$x_o = \mathcal{S}(\text{GNN}_L(\hat{x} | \theta), p_k^{\text{hyp}}), \quad (13)$$

where $\text{GNN}_L(\hat{x} | \theta)$ denotes the output of a L -layered GNN architecture with the trainable parameters θ , x is the input node features, x_o is the final output, and p_k^{hyp} is the hyperbolic PE of k^{th} category. *mathcal{G}* is the strategy for combining positional encodings and node features. As discussed earlier, the Euclidean node features and hyperbolic positional encodings can not be directly combined. Here, we can employ either HyPE or HyPEv2 as the combination strategy. In this way, the proposed framework solves both problem of Graph Transformers as well as deep GNNs.

3.9 Motivation behind choosing the Hyperbolic Space

Hyperbolic space is equipped with constant negative curvature where volume of a ball grows in exponential order with proportional to the radius. Unlike in Euclidean domain where volume of the ball grows in polynomial order because the space is free of curvature. Therefore, the input graphs can be embedded in the hyperbolic space with lower distortion comparing with the same in the Euclidean space. In addition, the embeddings in hyperbolic space preserves the neighborhood of the every vertex of the graph. In our framework, HyPE-GT learns positional encodings in the hyperbolic space which captures the complex patterns of the neighborhoods. Therefore, the positional encodings in the hyperbolic space might able to represent the topological positions corresponds to the nodes in the graph. Refer Figure 1 for detailed visualizations of the node embeddings in the hyperbolic space for both the variants of our framework. The learned PEs are integrated with the node features in the Euclidean space. Hence, embeddings in the hyperbolic space underscores the effectiveness of the positional encodings which will be fed to the Graph Transformer.

4 EXPERIMENTS AND RESULTS

4.1 Datasets

We evaluate the HyPE-GT and HyPE-GTv2 framework on several benchmark datasets. From Benchmarking GNNs [28] CLUSTER, PATTERN, MNIST, and CIFAR10 are selected for node-level and graph-level classification tasks. We run experiments on the ogbg-molhiv dataset from open graph benchmark (OGB) [32] as large-scale dataset. To measure the performance in deeper GNNs we consider co-author and co-purchase datasets [33]. The details of the datasets can be found in Section 1 of the supplementary material. The Pytorch and DGL-based implementation of the HyPE-GT framework is available at <https://github.com/kushalbose92/HyPE-GT>.

4.2 Results & Discussion

We perform a multitude of experiments to showcase the applicability of the proposed HyPE-GT framework on several graph datasets. We will resolve the following research questions through the empirical evidences. The experimental setup and details of hyper-parameters are provided in Section 2 and Section 3 respectively in the supplementary document.

RQ1. How do hyperbolic positional encodings improve the performance of the standard graph transformer ?

We have applied the HyPE-GT and HyPE-GTv2 frameworks on inductive node classification tasks on PATTERN and CLUSTER, graph classification of superpixel-based graphs MNIST and CIFAR10, and the binary classification task on the large-scale graph ogbg-molhiv. The experiments are performed in the mode of sparse graph settings. For each dataset, we perform experiments for 8 different types of hyperbolic positional encodings to demonstrate the significance of generating a diverse set of PEs. Refer to Table 1 for the numerical results of the PATTERN, CLUSTER, MNIST, and CIFAR10. Also refer to Table 2 for the numerical results on ogbg-molhiv dataset. The mean and standard deviations are reported after averaging the results of the 10 different runs on multiple random seeds. The performance metric for PATTERN, CLUSTER, MNIST, and CIFAR10 is accuracy, which is higher denotes the better. The metric of ogbg-molhiv is AUROC for which also a higher value indicates a better performance. The top three results are marked along with the number of hidden layers of either HGCN or HNN mentioned in the parenthesis.

HyPE-GT attains 3rd position on PATTERN dataset for PE category of 1 with a single-layered HGCN. The other variant HyPE-GTv2 performs poorly with respect to Transformer-based methods still outperforms GraphTransformer and other message-passing based methods. For CLUSTER, HyPE-GT again achieves 3rd position for PE category of 1 with a 1 layer HGCN. HyPE-GT on MNIST dataset, outperforms all existing Transformer-based methods as well as message-passing methods. The optimal result is obtained with PE category of 8 with a 2-layered HGCN model. In addition, HyPE-GTv2 achieves second position with PE category of 2 with a 2-layered HNN model. On CIFAR10, HyPE-GT attains 3rd position for the PE category of 7 with a 2-layered HGCN. The second variant also exhibits good performance by outperforming GCN, GAT and GIN. HyPE-GT shows superior performance on ogbg-molhiv by outperforming all other notable contenders. The best result is obtained for the PE category of 1 with a 2-layered HGCN model. The variant HyPE-GTv2 also showed commendable result with the PE category of 1 also with also a 2-layered HGCN. The results are the evident of the utility of generating multiple hyperbolic positional encodings which provides diverse scope for the optimal positional encodings. PATTERN and CLUSTER show optimal performance with the manifold type is Hyperboloid and for MNIST and CIFAR10 the same is PoincareBall.

RQ2. Can hyperbolic positional encodings improve the performances of deep GNN models ?

Graph Transformer leverages long-range interaction by measuring the attention among the node pairs which tackles over-smoothing issue to some extent. Still we want to explore the effect of incorporating hyperbolic positional encodings directly with the multi-layered graph convolution-based architectures. The generated positional encodings are flexibly integrated with the learned node features from the hidden layers to boost the model performance. We carry out a extensive experiment on co-purchase and co-author datasets Amazon Photo, Amazon Computers, Coauthor CS, and Coauthor Physics aim for solving the task of semi-supervised mode classification. Our experiment encompasses around the three well-adopted base GNN models like GCN [29], JKNet [34], and GCNII [35]. For every dataset, we apply each chosen base models. For each base GNN model, once we run experiments without using any positional encodings and in second phase HyPE and HyPEv2 are coupled with base models. The process is repeated for every network depth chosen from the set {2, 4, 8, 16, 32, 64, 128}. The numerical results are reported in Table 3. The performance is measured with the test accuracy which is obtained by taking the mean of the 10 different runs on multiple random seeds. We run experiments for all 8 categories and we only report the optimal one among them. The category of PE is also mentioned along with the highlighted test accuracy for both HyPE and HyPEv2.

The reported results are evident for the better applicability of the hyperbolic positional encodings integrating with deeper GNN architectures. The base models witnessed performance rise when associated with HyPE or HyPEv2 framework comparing with the performance of the GNN model without involving the positional encodings at almost every network depth. The optimal results are obtained for different categories of PEs which also indicates the benefits of generating a diverse set of hyperbolic positional encodings. The performance of vanilla GCN on all datasets significantly improves with the HyPE and HyPEv2 framework, especially with a network depth of more than 16 layers. On the other hand, JKNet and GCNII perform well on all four datasets except for Amazon Photo and Coauthor CS when network depth is more than 4. The minor performance degradation is observed only for HyPEv2 but for HyPE the performance is consistent. It can be concluded that HyPE is more powerful than HyPEv2. Again the performance improvement on GCNII and JKNet is lesser than GCN due to those models are designed for controlling over-smoothing but our framework still able to improve the performance with a good margin which denotes the capability of the proposed framework.

4.3 Selection Criteria of Positional Encodings

An obvious question will naturally arise how to determine optimal triplet from the set of positional encodings for solving the downstream tasks. We attempt to resolve the issue through analysing the experimental results. To avoid the time-consuming effort to search randomly the best positional encoding, we devised a intuitive strategy to minimise the search time. Our framework achieves optimal results on PATTERN, CLUSTER, CIFAR10, ogbg-molhiv when the PEs are learned via HGCN rather than HNN. Therefore, HGCN may be an appropriate candidate to initiate the search as it captures the

TABLE 2: Performance of ogbg-molhiv on HyPE-GT and HyPE-GTv2 are presented. The optimal result is reported which is the average of 10 different runs with standard deviation. An optimal number of layers are mentioned in the parenthesis. The top three results **first**, **second**, and **third** are marked.

Method	ogbg-molhiv
	AUROC \uparrow
GCN+virtual node	0.7599 \pm 0.0119
GIN+virtual node	0.7707 \pm 0.0149
DeeperGCN [36]	0.7858 \pm 0.0117
GSN(GIN+VN base) [37]	0.7799 \pm 0.0100
ExpC [38]	0.7799 \pm 0.0082
GraphTransformer [10]	0.7619 \pm 0.0141
SAN [5]	0.7785 \pm 0.2470
GraphGPS [13]	0.7880 \pm 0.0101
HyPE-GT (ours)	0.7893 \pm 0.0005(1, 2)
HyPE-GTv2 (ours)	0.7823 \pm 0.0103(1, 2)

structural patterns of the input graph. Only HyPE-GT on MNIST shows best performance when HNN is employed also the second best result occurred with HNN. Experiments suggest that Hyperboloid dominates over PoincareBall in most of the cases. Again LapPE and RWPE both works well in the experiments. We still recommend to perform exhaustive search to find the most effective positional encodings for the respective downstream tasks.

4.4 Depth of the Hyperbolic Networks in HyPE-GT

In this section, we studied the effect of the depth of the hyperbolic networks (both HNN and HGCN) on the performance of HyPE-GT. We include PATTERN, CLUSTER, MNIST, CIFAR10, and ogbg-molhiv to conduct the experiment. As HyPE-GT can generate 8 different types of hyperbolic positional encodings, we only focus on the categories which exhibit the best performance like HyPE-GT achieves the best on and MNIST and CIFAR10 for the categories of 8 and 7 respectively, where HyPE-GT obtained best performances on PATTERN and CLUSTER when the categories are both 1. On ogbg-molhiv, the framework performs the best when PE category is 1. We vary the number of layers of the hyperbolic networks from 1 – 5. For each network depth, we run experiments on the dataset with the fixed category of PE. We run the experiments for 4 times and plot the mean along with standrad deviations in Figure 4. The performance metric is also mentioned against each plot.

The performance of HyPE-GT deteriorates on datasets PATTERN, CLUSTER, CIFAR10, and ogbg-molhiv due to the over-smoothing issue in the hyperbolic graph convolutional-based architectures. Our framework shows poor performance on PATTERN and CLUSTER from the 2nd layer. But HyPE-GT develops peaks at the 2nd layer and after that performance gradually decreases. On the other hand, HyPE-GT consistently performs on MNIST due to the absence of over-smoothing issue in hyperbolic neural networks.

5 ABLATION STUDY

We perform detailed ablation study on both of our proposed variants HyPE-GT and HyPE-GTv2 to analyse the effect of individual modules of the proposed framework. We include all five datasets like PATTERN, CLUSTER, MNIST, CIFAR10, and ogbg-molhiv to carry out the experiment. We run the experiment for every category of positional encodings (as there are 8 possible PEs) for each of the dataset. For each category of PE, we separately run two variants by maintaining the similar hyper-parameters for the fair comparison. The results are presented in Figure 5. On PATTERN and CLUSTER dataset, for few categories of positional encodings, HyPE-GTv2 shows better performance than HyPE-GT. Again for rest of the categories of positional encodings HyPE-GTv2 exhibit more efficiency than HyPE-GTv2. This fact validates the capability of the individual variants for complementing each others’ performances. For MNIST and CIFAR10, the performances of both HyPE-GT and HyPE-GTv2 remains almost identical which demonstrates the comparative efficacy of the two variants. Furthermore, both HyPE-GT and HyPE-GTv2 on ogbg-molhiv exhibit identical strengths. Sometimes, HyPE-GTv2 outperforms than the HyPE-GT in some category of PEs.

6 CONCLUSION & FUTURE WORKS

In this work, we put forth a novel framework called HyPE-GT along with a variant HyPE-GTv2 to generate positional encodings in the hyperbolic space for graph transformers. Our framework is capable to generate a set of positional encodings which offers diverse choices to select the best one, unlike the other existing methods. The generated PEs are learned either by HNN or HGCN-based architectures. The efficiency of HyPE-GT is also validated by performing several experiments on molecular graphs from benchmark datasets [28] and OGB [32] graph datasets and achieving superior performances 2 out of 5 datasets. We provided results of exhaustive ablation study to substantiate the importance of each component of HyPE-GT and HyPE-GTv2. We also re-purpose the positional encodings for the nodes to boost the

TABLE 3: The performances of GCN, JKNet, and GCNII on co-author and co-purchase networks are presented for different depth of the networks coupled with HyPE and HyPEv2 framework. The best results are marked in green with category of PE is also mentioned in the parenthesis where optimal performance is achieved.

	Method / Layers	2	4	8	16	32	64	128	
Amazon Photo	GCN	85.57	84.44	51.53	49.78	52.74	52.92	50.54	
	GCN + HyPE	90.4(7)	80.54(8)	82.48(2)	81.24(3)	80.5(3)	80.91(3)	80.73(3)	
	GCN + HyPEv2	86.73(2)	85.63(8)	79.99(4)	79.77(3)	79.96(4)	79.71(2)	79.96(4)	
	JKNet	80.46	86.00	82.98	83.35	80.9	83.72	86.11	
	JKNet + HyPE	89.34(4)	90.87(4)	90.04(8)	89.67(8)	89.78(4)	89.56(4)	90.43(4)	
	JKNet + HyPEv2	87.75(4)	89.45(2)	87.49(7)	87.53(6)	87.19(2)	87.71(2)	87.96(7)	
	GCNII	83.13	86.92	85.39	87.45	85.82	86.06	86.08	
	GCNII + HyPE	91.1(8)	92.14(7)	92.07(7)	91.32(7)	91.43(8)	91.1(7)	91.48(7)	
	GCNII + HyPEv2	89.41(8)	85.75(6)	83.83(8)	82.19(6)	82.12(2)	82.26(4)	82.15(4)	
	Amazon Computers	GCN	69.94	67.55	49.0	49.38	48.6	49.55	48.66
		GCN + HyPE	82.61(8)	75.78(4)	72.86(3)	72.6(3)	73.97(3)	72.91(3)	73.75(3)
		GCN + HyPEv2	76.34(4)	73.47(3)	73.17(3)	73.56(3)	74.1(3)	74.32(3)	73.74(3)
JKNet		64.88	74.03	53.21	54.57	58.26	55.05	67.7	
JKNet + HyPE		80.03(5)	81.13(4)	76.86(4)	76.49(3)	75.8(3)	76.12(3)	75.63(3)	
JKNet + HyPEv2		77.75(4)	77.93(4)	76.21(4)	75.72(4)	73.94(2)	73.48(1)	74.9(3)	
GCNII		71.93	74.58	64.04	72.59	69.54	69.99	68.68	
GCNII + HyPE		82.66(8)	82.86(7)	81.48(7)	81.75(4)	80.55(7)	81.07(4)	80.75(7)	
GCNII + HyPEv2		77.88(4)	76.51(4)	75.77(4)	75.71(3)	75.32(2)	75.41(2)	74.62(2)	
Coauthor CS		GCN	89.89	83.83	16.42	15.37	12.01	21.36	11.66
		GCN + HyPE	92.09(8)	88.96(3)	82.58(4)	82.04(4)	82.16(3)	82.17(4)	81.52(3)
		GCN + HyPEv2	90.34(3)	87.06(3)	83.02(4)	82.3(4)	82.74(4)	82.44(2)	82.32(4)
	JKNet	91.45	89.5	89.05	87.99	88.39	87.6	87.28	
	JKNet + HyPE	92.64(2)	92.58(7)	92.11(4)	92.22(8)	92.31(8)	92.24(8)	92.17(7)	
	JKNet + HyPEv2	91.6(1)	89.9(3)	89.48(6)	90.27(1)	88.75(4)	89.05(1)	88.65(3)	
	GCNII	90.74	90.14	88.55	92.82	93.02	93.08	93.08	
	GCNII + HyPE	93.19(5)	93.01(8)	93.5(3)	93.65(3)	93.58(4)	93.68(4)	93.58(8)	
	GCNII + HyPEv2	91.95(2)	90.84(2)	89.96(2)	91.58(6)	91.95(6)	92.03(8)	91.88(8)	
	Coauthor Physics	GCN	93.9	90.97	89.46	51.81	52.96	49.29	51.8
		GCN + HyPE	94.26(4)	93.49(3)	90.26(4)	89.88(2)	90.16(4)	89.7(2)	90.01(2)
		GCN + HyPEv2	94.08(2)	93.26(2)	90.35(2)	90.5(2)	90.01(2)	90.25(2)	90.37(2)
JKNet		93.56	93.31	92.77	91.99	92.29	93.4	92.09	
JKNet + HyPE		94.23(7)	94.44(8)	94.23(7)	94.33(7)	93.93(5)	94.37(8)	94.23(8)	
JKNet + HyPEv2		93.79(8)	93.8(8)	93.92(8)	93.59(1)	93.27(5)	93.63(7)	93.72(8)	
GCNII		94.0	93.54	93.97	94.1	94.24	94.03	94.02	
GCNII + HyPE		94.37(3)	94.45(4)	94.6(6)	94.62(3)	94.53(4)	94.43(3)	94.76(6)	
GCNII + HyPEv2		94.27(2)	93.9(4)	94.19(2)	94.43(4)	94.41(4)	94.43(2)	94.43(2)	

performance of deep graph neural networks applied on Co-author and Co-purchase datasets. As a future work, it may be beneficial to explore various design choices of the modules of HyPE that produce multiple set of hyperbolic PEs. Also, how to use positional encodings in deeper GNN architectures in more efficiently further investigation is required.

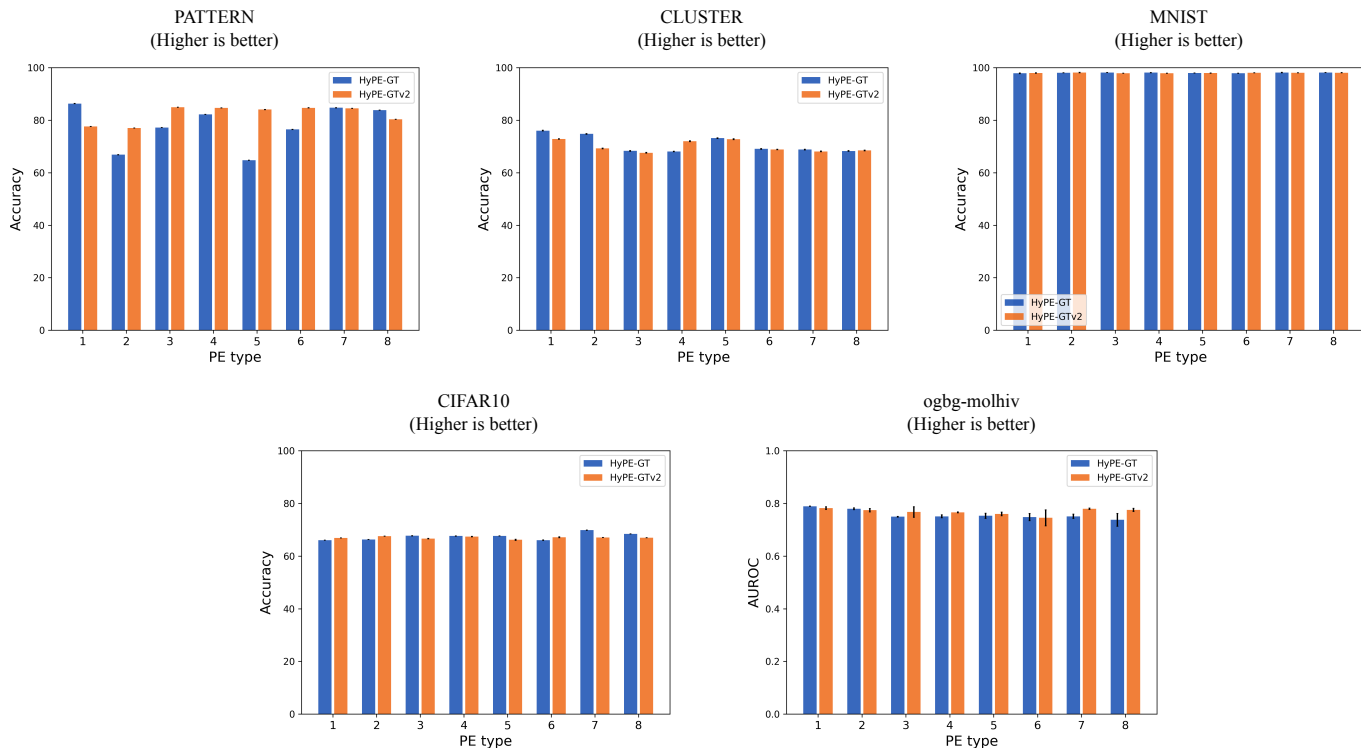


Fig. 5: The comparative study of the performances of HyPE-GT and HyPE-GTv2 are presented for all categories of hyperbolic positional encodings. on all five benchmark datasets.

7 DETAILS OF THE DATASETS

TABLE 4: Details of the datasets from [28] and [32]

Name	#Graphs	Avg # Nodes	Avg # Edges	Task	Directed	Metric
PATTERN	14000	118.9	3,039.3	binary classif.	No	Accuracy
CLUSTER	12000	117.2	2,150.9	6-class classif.	No	Accuracy
MNIST	70,000	70.6	564.5	10-class classification	Accuracy	Accuracy
CIFAR10	60,000	117.6	941.1	10-class classification	Accuracy	Accuracy
ogbg-molhiv	41127	25.5	27.5	binary classif.	No	AUROC

TABLE 5: Details of the Co-author and Co-purchase datasets

Dataset	Nodes	Edges	Features	Classes
Amazon photo	13752	491722	10	767
Amazon Computers	7650	238162	8	745
Coauthor CS	18333	81894	15	6805
Coauthor Physics	34493	495924	5	8415

PATTERN and **CLUSTER** are molecular datasets generated from Stochastic Block Model [39]. The prediction task here is an inductive node-level classification. In **PATTERN** the task is to identify which nodes in a graph belong to one of 100 different sub-graph patterns which were randomly generated with different SBM parameters. In **CLUSTER**, every graph is composed of 6 SBM-generated clusters, each drawn from the same distribution, with only a single node per cluster containing a unique cluster ID. Our target is predict the cluster ID of the nodes.

MNIST and **CIFAR10** are generated from image classification datasets of similar names. Superpixel datasets are constructed by an 8 nearest-neighbor graph of SLIC superpixels for each image. The 10-class classification tasks and standard dataset splits follow the original image classification datasets, i.e., for MNIST 55K/5K/10K and for CIFAR10 45K/5K/10K train/validation/test graphs.

ogbg-molhiv are molecular property prediction datasets designed by OGB from MoleculeNet. The molecules are represented by the nodes (atom) and edges (bond). The node and edge features are generated from similar source which represents chemo-physical properties. The prediction task of ogbg-molhiv is the binary classification of the molecule’s suitability for combating the replication of HIV.

Co-authorship datasets Coauthor CS and Coauthor Physics are two co-authorship networks [33]. Nodes represent authors and edges exist between them if they co-authored a paper. The features of the nodes represent the keywords related to the paper of the author. Label of the each node denotes field of the study of the corresponding author.

Co-purchase datasets Amazon Computers and Amazon Photo are two co-purchase networks [33] where each node denotes products and edge exists if two products are bought frequently. Node features denote the bag-of-words representation of the product reviews. Node labels indicate the product category.

8 EXPERIMENTAL SETUP

We run the experiments on the datasets with the standard train/validation/test splits. The mean and standard deviations are reported after 10 runs on multiple random seeds for each dataset. All experiments are done on a single GPU GeForce RTX 3090 with 24GB memory capacity.

9 HYPERPARAMETER DETAILS

In this section, we will provide detailed description of the hyper-parameters of every dataset which are employed for the experimentation. Refer Tables 6, 7, 8, 9, and 10 for the hyper-parameters of category-wise positional encodings for MNIST, CIFAR10, PATTERN, CLUSTER, and ogbg-molhiv datasets respectively. The hyper-parameters are adjusted from the initial setting which are inspired from SAN [5], GraphGPS [13], SAT [6], and GraphGPS [13]. We keep similar for both variants HyPE-GT and HyPE-GTv2. The model parameters are optimized by Adam [40] optimizer with the default settings. The learning rate is adjusted after the number of "patience" epochs.

The hyperparameters of the Co-author and Co-purchase datasets are provided in Table 11. The dimension of positional vector is 128 when PEs are initialized by the eigenvectors of Laplacian matrix for every network depth. The dimension of PE is fixed at 8 when PEs are initialized with RWPE.

TABLE 6: Hyperparameters for MNIST dataset for every category of PE generated in the experiments.

Hyperparameters / PE Category	MNIST							
	1	2	3	4	5	6	7	8
# HyPE-GT Layers				4				
# Head				8				
Hidden Dim				80				
Curvature				1.0				
Activation				ReLU				
# PE Layers				2				
Dropout				0.0				
Layernorm				False				
Batchnorm				True				
PE Dim				6				
Graph Pooling				Mean				
Batch size				128				
Init LR				0.001				
Epochs				1000				
Patience				10				
Weight Decay				0.0				

TABLE 7: Hyperparameters for CIFAR10 dataset for every category of PE generated in the experiments.

Hyperparameters / PE Category	CIFAR10							
	1	2	3	4	5	6	7	8
# HyPE-GT Layers				4				
# Head				8				
Hidden Dim				80				
Curvature				1.0				
Activation				ReLU				
# PE Layers				2				
Dropout				0.0				
Layernorm				False				
Batchnorm				True				
PE Dim				16				
Graph Pooling				Mean				
Batch size				128				
Init LR				0.001				
Epochs				1000				
Patience				10				
Weight Decay				0.0				

TABLE 8: Hyperparameters for PATTERN dataset for every category of PE generated in the experiments.

Hyperparameters / PE Category	PATTERN							
	1	2	3	4	5	6	7	8
# HyPE-GT Layers		10				10		
# Head		8				8		
Hidden Dim		80				80		
Curvature		1.0				1.0		
Activation		ReLU				ReLU		
# PE Layers		1				1		
Dropout		0.0				0.0		
Layernorm		False				False		
Batchnorm		True				True		
PE Dim		6				2		
Graph Pooling		Mean				Mean		
Batch size		26				26		
Init LR		0.0005				0.0003		
Epochs		1000				1000		
Patience		10				10		
Weight Decay		0.0				0.0		

TABLE 9: Hyperparameters for CLUSTER dataset for every category of PE generated in the experiments.

Hyperparameters / PE Category	CLUSTER							
	1	2	3	4	5	6	7	8
# HyPE-GT Layers		10				10		
# Head		8				8		
Hidden Dim		80				80		
Curvature		1.0				1.0		
Activation		ReLU				ReLU		
# PE Layers		4				2		
Dropout		0.0				0.0		
Layernorm		False				False		
Batchnorm		True				True		
PE Dim		6				16		
Graph Pooling		Mean				Mean		
Batch size		32				32		
Init LR		0.0005				0.0003		
Epochs		1000				1000		
Patience		10				10		
Weight Decay		0.0				0.0		

TABLE 10: Hyperparameters for ogbg-molhiv dataset for every category of PE generated in the experiments.

Hyperparameters / PE Category	ogbg-molhiv							
	1	2	3	4	5	6	7	8
# HyPE-GT Layers					10			
# Head					4			
Hidden Dim					64			
Curvature					1.0			
Activation					ReLU			
# PE Layers					2			
Dropout					0.01			
Layernorm					False			
Batchnorm					True			
PE Dim					32			
Graph Pooling					Mean			
Batch size					64			
Init LR					0.0001			
Epochs					1000			
Patience					20			
Weight Decay					0.0			

TABLE 11: Hyperparameters for Co-author and Co-purchase datasets

Hyperparameters	Amazon photo	Amazon computers	Coauthor CS	Coauthor Physics
Learning rate	0.01	0.01	0.01	0.01
PE Dim	128/8	128/8	128/8	128/8
Hidden Dim	64	64	64	64
#PE Layers	2	2	2	2
Activation	ReLU	ReLU	ReLU	ReLU
Dropout	0.50	0.50	0.20	0.20
Curvature	1.0	1.0	1.0	1.0
weight decay	0.0005	0.0005	0.0005	0.0005
Training Epochs	500	500	500	500

10 MORE RESULTS ON CO-AUTHOR AND CO-PURCHASE DATASETS

We reuse hyperbolic positional encodings to improve the performance of the multi-layered deep models. We perform extensive experiments on Amazon photo, Amazon computers, Coauthor CS, and Coauthor Physics datasets to show the capability of hyperbolic coordinates. Refer Tables 12, 13, 14, and 15 for the detailed performances analysis. We have two columns against each layer which denotes results obtained from HyPE and HyPEv2 respectively. Each result is obtained by taking mean of the 10 runs on multiple random seeds. We have omitted the standard deviations due to the space limitations. The numerical results clearly indicate the utility of generating multiple categories of positional encodings. The GNN models like GCN [29], JKNet [34], and GCNII [35] associated with HyPE outperforms the performance of the base models by at least one of the category of PE for each variant.

11 COMPARATIVE STUDY ON NUMBER OF PARAMETERS

We perform a comparative study on the parameters of the existing Graph Transformers like GraphTransformer [10], SAN [5], SAT [6], Graphormer [7], EGT [15], and GraphGPS [13] with our proposed method HyPE-GT. Refer Table ?? for the detailed information regarding the number of model parameters. The number of parameters for both variants are equal because variants are structurally identical but they differ only the way PEs are incorporated. For PATTERN and CLUSTER, our both variants has the number of parameters comparable with GraphTransformer, SAN, and RGT. But as GraphGPS is a linearized Transformer architecture. Therefore, it is desirable to have lower number of parameters. But SAT have much higher number of parameters. On the other side, our framework produces higher number of parameters compared to EGT and GraphGPS (as rest of the methods do not report the numbers). Still HyPE-GT outperforms all methods. Lastly, our framework produces lowest number of parameters compared to all SOTA approaches and also it achieves best performance on the dataset. As ogbg-molhiv is one of the large-scale graphs and the performance of the framework is the evidence of the power of the hyperbolic positional encodings.

REFERENCES

- [1] Q. Li, Z. Han, and X.-M. Wu, "Deeper insights into graph convolutional networks for semi-supervised learning," in *Thirty-Second AAAI conference on artificial intelligence*, 2018.
- [2] U. Alon and E. Yahav, "On the bottleneck of graph neural networks and its practical implications," *arXiv preprint arXiv:2006.05205*, 2020.
- [3] K. Xu, W. Hu, J. Leskovec, and S. Jegelka, "How powerful are graph neural networks?" *arXiv preprint arXiv:1810.00826*, 2018.
- [4] C. Morris, M. Ritzert, M. Fey, W. L. Hamilton, J. E. Lenssen, G. Rattan, and M. Grohe, "Weisfeiler and leman go neural: Higher-order graph neural networks," in *Proceedings of the AAAI conference on artificial intelligence*, vol. 33, no. 01, 2019, pp. 4602–4609.
- [5] D. Kreuzer, D. Beaini, W. Hamilton, V. Létourneau, and P. Tossou, "Rethinking graph transformers with spectral attention," *Advances in Neural Information Processing Systems*, vol. 34, pp. 21 618–21 629, 2021.

TABLE 12: The complete results for Amazon Photo for both HyPE and HyPEv2 are presented. The best results are boldfaced.

Amazon Photo																	
Method	Init PE	Hyperbolic Manifold	Hyperbolic NN	2		4		8		16		32		64		128	
GCN				85.57		84.44		51.53		49.78		52.74		52.92		50.54	
GCN + HyPE	LapPE	Hyperboloid	HGCN	88.22	78.14	57.99	78.12	54.14	78.74	51.35	78.14	56.21	78.63	55.82	78.68	70.21	78.81
			HNN	85.27	86.73	86	84.79	82.48	79.56	79.2	79.63	79.21	79.43	78.26	79.71	80.08	79.59
		PoincareBall	HGCN	83.38	81.45	80.55	80.17	81.05	79.34	81.24	79.77	80.5	79.32	80.91	79.39	80.73	79.48
			HNN	90.01	85.82	83.23	83.78	80.88	79.99	80.72	79.46	80.3	79.96	80.43	79.5	80.17	79.96
	RWPE	Hyperboloid	HGCN	87.81	82.47	71.08	46.69	46.17	48.58	50.43	61.45	49.48	47.09	50.95	49.71	51.27	50.37
			HNN	87.23	85.85	85.01	82.48	50.01	54.33	54.34	50.95	58.23	52.37	56.44	53.5	49.34	51.17
		PoincareBall	HGCN	90.4	85.52	85.78	83.32	70.37	58.12	55.79	60.69	58.86	57.3	60.55	57.6	59.31	51.61
			HNN	89.72	85.46	86.54	85.63	81.43	48.37	55.26	52.01	59.01	51.43	57.38	50.55	52.14	52.37
JKNet				80.46		86		82.98		83.35		80.9		83.72		86.11	
JKNet + HyPE	LapPE	Hyperboloid	HGCN	86.32	79.83	57.66	79.6	56.5	80.21	58.08	80.3	55.77	80.19	54.06	80.3	53.42	80.4
			HNN	86.44	86.06	87.45	89.45	83.85	86.61	81.28	86.7	80.54	87.19	81.01	87.71	81.13	86.79
		PoincareBall	HGCN	82.26	80.39	83.09	82.68	82.34	80.11	82.44	80.07	82.57	80.25	82.88	80.34	82.32	80.01
			HNN	89.34	87.75	90.87	88.06	89.32	86.8	89.59	86.26	89.78	85.9	89.56	84.52	90.43	86.23
	RWPE	Hyperboloid	HGCN	87.19	82.99	88.37	78.01	40.69	86.5	40.87	78.74	39.7	80.8	38.23	80.68	36.79	47.7
			HNN	86.41	87.61	86.3	86.66	87.13	87.41	78.51	87.53	77.53	84.06	83.7	87.42	61.43	82.44
		PoincareBall	HGCN	88.4	82.48	90.43	85.99	90.01	87.49	89.16	83.77	89.32	86.04	87.93	82.41	89.24	87.96
			HNN	87.64	81.85	89.92	86.1	90.04	86.83	89.67	86.55	88.08	86.68	87.16	87.09	86.91	86.3
GCNII				83.13		86.92		85.39		87.45		85.82		86.06		86.08	
GCNII + HyPE-GT	LapPE	Hyperboloid	HGCN	89.4	79.3	90.57	79.88	89.66	80.04	86.95	79.72	86.99	79.66	87.19	79.81	87.01	79.68
			HNN	88.88	85.2	90.32	83.88	85.1	81.86	81.92	82.15	81.9	82.12	81.56	81.83	86.1	81.85
		PoincareBall	HGCN	81.17	79.53	81.12	79.5	80.88	79.89	81.19	80.48	80.9	79.92	80.91	79.59	81.32	79.74
			HNN	90.29	85.35	90.33	84.3	86.11	81.74	85.86	82.14	86.91	81.85	86.97	82.26	87.13	82.15
	RWPE	Hyperboloid	HGCN	90.74	73.38	88.23	74.41	88.73	73.59	86.59	62.47	85.48	64.8	87.06	57.53	86.4	60.22
			HNN	90.21	84.3	85.7	85.75	86.44	82.51	86.86	82.19	86.23	79.5	86.03	80.37	85.63	80.33
		PoincareBall	HGCN	90.92	85.13	92.14	84.59	92.07	76.07	91.32	69.16	91.37	69.49	91.1	70.29	91.48	86.08
			HNN	91.1	89.41	91.59	84.98	91.85	83.83	91.17	82.12	91.43	80	90.48	78.26	90.55	80.55

TABLE 13: The complete results for Amazon Computers for both HyPE and HyPEv2 are presented. The best results are boldfaced.

Amazon Computers																	
Method	Init PE	Hyperbolic Manifold	Hyperbolic NN	2		4		8		16		32		64		128	
GCN				69.94		67.55		49		49.38		48.6		49.55		48.66	
GCN + HyPE	LapPE	Hyperboloid	HGCN	78.36	72.37	53.11	70.61	50.85	71.51	46.16	72.24	53.88	72.34	38.36	7.64	44.89	71.51
			HNN	75.12	76.1	69.24	69.83	67.97	69.78	67.63	68.76	69.15	71.46	69.73	69.96	68.74	71.57
		PoincareBall	HGCN	79.04	72.83	73.48	73.47	72.86	73.17	72.6	73.56	73.97	74.1	72.91	74.31	73.75	73.74
			HNN	79.68	76.34	75.78	72.76	71.19	71.96	71.66	69.63	73.04	71.56	72.38	69.84	72.28	70.21
	RWPE	Hyperboloid	HGCN	76.92	72.19	70.56	37.13	50.95	36.65	49.69	46.33	50.78	41.95	50.36	40.86	39.69	46.34
			HNN	77.95	70.79	66.41	69.9	47.62	42.6	48.71	48.68	51.5	47.34	42.56	46.71	43.91	47.56
		PoincareBall	HGCN	81.42	75.2	70.04	70.68	50.22	52.63	55.09	53.33	53.75	52.04	51.61	50.45	54.51	53.58
			HNN	82.61	72.31	69.08	64.55	51.13	49.06	51.49	47.52	50.78	50.17	52.29	45.42	54.26	51.34
JKNet				64.88		74.03		53.21		54.57		58.26		55.05		67.7	
JKNet + HyPE	LapPE	Hyperboloid	HGCN	76.66	73.31	79.14	73.03	68.52	72.74	59.65	73.57	46.54	71.78	55.55	73.48	53.32	72.2
			HNN	71.02	76.98	72.73	76.47	74	77.48	70.86	74.35	70.56	73.94	73.79	71.7	73.03	72.46
		PoincareBall	HGCN	75.26	73.32	77.32	73.81	75.98	74.14	76.49	73.4	75.8	73.54	76.12	72.96	75.63	74.9
			HNN	74.15	77.75	81.13	77.93	76.86	76.21	75.62	75.72	74.03	73.81	72.59	72.99	72.43	71.63
	RWPE	Hyperboloid	HGCN	80.03	53.12	75.88	62.32	69.73	56.35	44.54	65.73	46.56	65.19	61.2	55.8	45.42	51.28
			HNN	72.62	64.47	63.93	73.08	46.59	62.16	49.74	62.17	46.29	67.46	49.15	63.82	42.97	57.67
		PoincareBall	HGCN	76.8	64.62	76.55	64.67	73.82	58.62	72.62	66.32	74.49	59.73	74.23	54.88	73.15	59.19
			HNN	75.17	67.69	79.78	74.7	74.35	66.34	73.91	66.19	72.28	62.23	73.75	57.38	72.68	55.73
GCNII				71.93		74.58		64.04		72.59		69.54		69.99		68.68	
GCNII + HyPE-GT	LapPE	Hyperboloid	HGCN	81.1	74.16	63.37	73.74	52.57	72.45	74.92	73.63	75.06	72.64	74.19	74.82	73.53	73.08
			HNN	80.92	77.37	71.72	76.44	72.61	74.71	73.39	74.98	72.91	75.32	72.88	75.41	72.53	74.62
		PoincareBall	HGCN	76.55	75.28	74.87	74.28	75.45	74.43	75.16	75.71	72.99	74.06	74.74	75	74.14	73.32
			HNN	83.64	77.88	82.21	76.51	81.35	75.77	81.75	74.72	80.25	74.18	81.07	74.39	79.86	74.27
	RWPE	Hyperboloid	HGCN	73.33	71.54	65.07	52.17	68.2	58.31	74.81	45.91	74.37	42.91	73.9	40.79	72.65	38.94
			HNN	73.51	73.13	67.78	73.31	68.1	62.75	73.72	62.75	73.69	58.05	71.93	60.12	71.94	58.45
		PoincareBall	HGCN	82.53	72.63	82.86	67.45	81.48	61.52	81.3	57.53	80.55	49.77	80.16	53.67	80.75	49.89
			HNN	82.66	70.72	81.9	68.5	80.54	62.87	80.87	64.45	79.95	60.63	79.95	58.96	79.32	57.96

TABLE 14: The complete results for Coauthor CS for both HyPE and HyPEv2 are presented. The best results are boldfaced.

Coauthor CS																	
Method	Init PE	Hyperbolic Manifold	Hyperbolic NN	2		4		8		16		32		64		128	
GCN				89.89		83.83		16.42		15.37		12.01		21.36		11.66	
GCN + HyPE	LapPE	Hyperboloid	HGCN	90.88	90.34	87.57	86.75	69.78	81.56	66.59	80.8	67.53	81.3	70.33	81.4	68.44	81.57
			HNN	91.19	90.06	80.67	85.25	78.69	82.61	79.48	81.94	80.35	82.39	80.28	82.44	81.25	82.08
		PoincareBall	HGCN	91.87	90.34	88.96	87.06	81.64	81.78	81.64	81.71	82.16	81.5	81.59	81.38	81.52	81.59
			HNN	91.8	90.07	86.35	82.7	82.58	83.02	82.04	82.3	81.69	82.74	82.77	82.27	81.21	82.32
	RWPE	Hyperboloid	HGCN	91.68	86.71	81.52	82.92	7.7	12.88	7.6	14.02	20.92	13.21	81.17	12.28	23.13	14.99
			HNN	91.37	90	82.75	83.9	9.99	9.91	22.92	12.03	22.48	11.15	10.09	10.39	23.03	15.7
		PoincareBall	HGCN	92.04	89.68	88.93	82.83	13.65	13.34	13.23	12.37	17.85	21.92	12.56	12.96	22.53	14.02
			HNN	92.09	89.85	88.22	81.96	11.28	12.27	11.86	9.92	13.27	21.27	11.59	12.08	15.42	11.17
JKNet				91.45		89.5		89.05		87.99		88.39		87.6		87.28	
JKNet + HyPE	LapPE	Hyperboloid	HGCN	92.32	91.6	91.16	88.78	90.14	88.73	90.6	90.27	91.18	88.39	91.29	89.05	90.89	86.5
			HNN														

TABLE 15: The complete results for Coauthor Physics for both HyPE and HyPEv2 are presented. The best results are boldfaced.

		Coauthor Physics															
Method	Init PE	Hyperbolic Manifold	Hyperbolic NN	2		4		8		16		32		64		128	
GCN				93.9		90.97		89.46		51.81		52.96		49.29		51.8	
GCN + HyPE	LapPE	Hyperboloid	HGCN	93.74	93.06	93.32	92.49	78.82	87.52	78.88	88.25	80.44	88.12	80.69	88.16	81.09	87.69
			HNN	93.95	94.08	93.04	93.26	89.89	90.35	89.88	90.5	89.97	90.01	89.7	90.25	90.01	90.37
		PoincareBall	HGCN	94.17	92.86	93.49	93.2	88.83	87.76	88.78	87.84	89.05	87.97	88.86	88.06	88.83	88.25
	RWPE	Hyperboloid	HGCN	94.26	94.04	93.33	92.34	90.26	90.26	89.41	89.91	90.16	89.88	89.59	90.06	89.36	89.95
			HNN	94	92.87	92.96	91.95	39.65	56.9	49.93	58.76	50.52	55.76	43.36	56.19	41.7	55.87
		PoincareBall	HGCN	94.26	93.58	93.01	91.81	88.63	50.29	49.36	51.7	55.44	48.44	54.07	50.23	51.03	51.08
JKNet	LapPE	Hyperboloid	HGCN	93.89	93.39	92.89	90.3	89.24	50.19	51.12	49.5	52.71	52.63	50.67	51.97	51.61	52.05
			HNN	93.56		93.31		92.77		91.99		92.29		93.4		92.09	
		PoincareBall	HGCN	93.71	93.6	93.67	92.94	93.54	93.25	93.7	93.59	93.39	93	93.8	93.07	93.47	92.12
	RWPE	Hyperboloid	HGCN	93.91	93.68	93.72	93.54	93.07	92.92	93.2	92.5	93.37	91.61	93.13	92.3	92.88	91.92
			HNN	93.95	93.56	93.79	93.09	93.77	93.29	93.68	92.83	93.61	92.64	93.37	91.94	93.57	92.37
		PoincareBall	HGCN	93.71	93.62	93.81	93.43	93.66	91.02	92.97	92.93	93.39	91.83	93.14	91.39	93.04	92.44
RWPE	Hyperboloid	HGCN	93.84	93.4	94.05	93.6	94.17	93.22	93.52	92.8	93.93	93.27	93.79	92.62	93.87	92.89	
		HNN	93.92	93.32	93.97	93.5	93.98	93.25	93.91	93.2	93.82	92.91	93.91	93.47	94.19	93.13	
	PoincareBall	HGCN	94.23	93.65	94.12	93.62	94.23	93.46	94.33	92.93	93.8	93.14	94.34	93.63	94.1	93.35	
GCNII	LapPE	Hyperboloid	HGCN	94.09	93.79	94.44	93.8	94.04	93.92	94.05	93.21	93.9	93.2	94.37	93.6	94.23	93.72
			HNN	94		93.54		93.97		94.1		94.24		94.03		94.02	
		PoincareBall	HGCN	94.09	93.47	94.36	92.94	94.45	91.04	94.37	90.89	94.45	90.76	94.41	91.13	94.64	90.8
	RWPE	Hyperboloid	HGCN	94.25	94.27	94.24	93.94	94.24	94.19	94.41	94.41	94.42	94.36	94.15	94.43	94.59	94.43
			HNN	94.37	93.35	94.38	92.93	94.43	91.43	94.62	90.4	94.53	90.64	94.43	90.62	94.74	90.56
		PoincareBall	HGCN	94.22	94.17	94.45	93.9	94.37	94	94.43	94.43	94.53	94.41	94.42	94.25	94.81	94.3
RWPE	Hyperboloid	HGCN	93.91	93.86	94.37	92.93	94.58	93.2	94.36	93.12	94.38	93.6	94.33	93.58	94.64	93.71	
		HNN	93.93	93.77	94.41	92.5	94.6	92.8	93.89	93.23	94.14	93.08	94.05	92.64	94.76	92.89	
	PoincareBall	HGCN	94.23	93.77	94.34	93.3	94.25	93	94.22	93.69	94.49	93.1	94.16	93.12	94.73	92.8	
GCNII + HyPE-GT	LapPE	Hyperboloid	HGCN	94.13	93.79	94.37	93.2	94.29	93.04	94.13	93.1	94.35	92.96	94.32	93.04	94.64	93.08
			HNN	94.09	93.79	94.37	93.2	94.29	93.04	94.13	93.1	94.35	92.96	94.32	93.04	94.64	93.08
		PoincareBall	HGCN	94.09	93.47	94.36	92.94	94.45	91.04	94.37	90.89	94.45	90.76	94.41	91.13	94.64	90.8
	RWPE	Hyperboloid	HGCN	94.25	94.27	94.24	93.94	94.24	94.19	94.41	94.41	94.42	94.36	94.15	94.43	94.59	94.43
			HNN	94.37	93.35	94.38	92.93	94.43	91.43	94.62	90.4	94.53	90.64	94.43	90.62	94.74	90.56
		PoincareBall	HGCN	94.22	94.17	94.45	93.9	94.37	94	94.43	94.43	94.53	94.41	94.42	94.25	94.81	94.3

TABLE 16: A comparative study on the number of parameters of HyPE-GT and HyPE-GTv2 with the other existing Graph Transformers.

Method / Data	Init PE	Hyperbolic Manifold	Hyperbolic NN	PATTERN	CLUSTER	MNIST	CIFAR10	ogbg-molhiv
GraphTransformer [10]				523146	522742	-	-	-
SAN [5]				507,202	519,186	-	-	528265
Graphormer [7]				-	-	-	-	47.0M
SAT [6]				825,986	741,990	-	-	-
EGT [15]				500000	500000	100000	100000	110.8M
GraphGPS [13]				337201	502054	115,394	112,726	558625
HyPE-GT / HyPE-GTv2 (ours)	LapPE	Hyperboloid	HGCN	524022	524426	369390	371150	389441
			HNN	523382	524426	369390	369550	390465
		Poincare Ball	HGCN	523382	524426	369390	369550	388929
			HNN	523382	524666	369390	369550	388929
	RWPE	Hyperboloid	HGCN	523142	524666	368830	368990	390465
			HNN	523142	524666	368830	368990	390465
		Poincare Ball	HGCN	523142	524666	368830	369790	390465
			HNN	524426	524666	368830	369790	390465

- [6] D. Chen, L. O’Bray, and K. Borgwardt, “Structure-aware transformer for graph representation learning,” in *International Conference on Machine Learning*. PMLR, 2022, pp. 3469–3489.
- [7] C. Ying, T. Cai, S. Luo, S. Zheng, G. Ke, D. He, Y. Shen, and T.-Y. Liu, “Do transformers really perform badly for graph representation?” *Advances in Neural Information Processing Systems*, vol. 34, pp. 28 877–28 888, 2021.
- [8] V. P. Dwivedi, A. T. Luu, T. Laurent, Y. Bengio, and X. Bresson, “Graph neural networks with learnable structural and positional representations,” *arXiv preprint arXiv:2110.07875*, 2021.
- [9] P. Veličković, G. Cucurull, A. Casanova, A. Romero, P. Lio, and Y. Bengio, “Graph attention networks,” *arXiv preprint arXiv:1710.10903*, 2017.
- [10] V. P. Dwivedi and X. Bresson, “A generalization of transformer networks to graphs,” *arXiv preprint arXiv:2012.09699*, 2020.
- [11] G. Mialon, D. Chen, M. Selosse, and J. Mairal, “Graphit: Encoding graph structure in transformers,” *arXiv preprint arXiv:2106.05667*, 2021.
- [12] Z. Wu, P. Jain, M. Wright, A. Mirhoseini, J. E. Gonzalez, and I. Stoica, “Representing long-range context for graph neural networks with global attention,” *Advances in Neural Information Processing Systems*, vol. 34, pp. 13 266–13 279, 2021.
- [13] L. Rampásek, M. Galkin, V. P. Dwivedi, A. T. Luu, G. Wolf, and D. Beaini, “Recipe for a general, powerful, scalable graph transformer,” *Advances in Neural Information Processing Systems*, vol. 35, pp. 14 501–14 515, 2022.
- [14] J. Kim, D. Nguyen, S. Min, S. Cho, M. Lee, H. Lee, and S. Hong, “Pure transformers are powerful graph learners,” *Advances in Neural Information Processing Systems*, vol. 35, pp. 14 582–14 595, 2022.
- [15] M. S. Hussain, M. J. Zaki, and D. Subramanian, “Global self-attention as a replacement for graph convolution,” in *Proceedings of the 28th ACM SIGKDD Conference on Knowledge Discovery and Data Mining*, 2022, pp. 655–665.
- [16] S. Yun, M. Jeong, R. Kim, J. Kang, and H. J. Kim, “Graph transformer networks,” *Advances in neural information processing systems*, vol. 32, 2019.
- [17] Z. Hu, Y. Dong, K. Wang, and Y. Sun, “Heterogeneous graph transformer,” in *Proceedings of the web conference 2020*, 2020, pp. 2704–2710.
- [18] O. Ganea, G. Bécigneul, and T. Hofmann, “Hyperbolic neural networks,” *Advances in neural information processing systems*, vol. 31, 2018.
- [19] V. Khulkov, L. Mirvakhabova, E. Ustinova, I. Oseledets, and V. Lempitsky, “Hyperbolic image embeddings,” in *Proceedings of the IEEE/CVF Conference on Computer Vision and Pattern Recognition*, 2020, pp. 6418–6428.
- [20] Q. Liu, M. Nickel, and D. Kiela, “Hyperbolic graph neural networks,” *Advances in neural information processing systems*, vol. 32, 2019.
- [21] I. Chami, Z. Ying, C. Ré, and J. Leskovec, “Hyperbolic graph convolutional neural networks,” *Advances in neural information processing systems*, vol. 32, 2019.

- [22] Y. Zhang, X. Wang, C. Shi, X. Jiang, and Y. Ye, "Hyperbolic graph attention network," *IEEE Transactions on Big Data*, vol. 8, no. 6, pp. 1690–1701, 2021.
- [23] A. Vaswani, N. Shazeer, N. Parmar, J. Uszkoreit, L. Jones, A. N. Gomez, L. u. Kaiser, and I. Polosukhin, "Attention is all you need," in *Advances in Neural Information Processing Systems*, I. Guyon, U. V. Luxburg, S. Bengio, H. Wallach, R. Fergus, S. Vishwanathan, and R. Garnett, Eds., vol. 30. Curran Associates, Inc., 2017. [Online]. Available: https://proceedings.neurips.cc/paper_files/paper/2017/file/3f5ee243547dee91fbd053c1c4a845aa-Paper.pdf
- [24] S. Ioffe and C. Szegedy, "Batch normalization: Accelerating deep network training by reducing internal covariate shift," in *International conference on machine learning*. pmlr, 2015, pp. 448–456.
- [25] J. L. Ba, J. R. Kiros, and G. E. Hinton, "Layer normalization," *arXiv preprint arXiv:1607.06450*, 2016.
- [26] K. Zhou, X. Huang, Y. Li, D. Zha, R. Chen, and X. Hu, "Towards deeper graph neural networks with differentiable group normalization," *arXiv preprint arXiv:2006.06972*, 2020.
- [27] P. Li, Y. Wang, H. Wang, and J. Leskovec, "Distance encoding: Design provably more powerful neural networks for graph representation learning," *Advances in Neural Information Processing Systems*, vol. 33, pp. 4465–4478, 2020.
- [28] V. P. Dwivedi, C. K. Joshi, T. Laurent, Y. Bengio, and X. Bresson, "Benchmarking graph neural networks," 2020.
- [29] T. N. Kipf and M. Welling, "Semi-supervised classification with graph convolutional networks," *arXiv preprint arXiv:1609.02907*, 2016.
- [30] X. Bresson and T. Laurent, "Residual gated graph convnets," *arXiv preprint arXiv:1711.07553*, 2017.
- [31] G. Corso, L. Cavalleri, D. Beaini, P. Liò, and P. Veličković, "Principal neighbourhood aggregation for graph nets," *Advances in Neural Information Processing Systems*, vol. 33, pp. 13 260–13 271, 2020.
- [32] W. Hu, M. Fey, M. Zitnik, Y. Dong, H. Ren, B. Liu, M. Catasta, and J. Leskovec, "Open graph benchmark: Datasets for machine learning on graphs," *arXiv preprint arXiv:2005.00687*, 2020.
- [33] O. Shchur, M. Mumme, A. Bojchevski, and S. Günnemann, "Pitfalls of graph neural network evaluation," *arXiv preprint arXiv:1811.05868*, 2018.
- [34] K. Xu, C. Li, Y. Tian, T. Sonobe, K.-i. Kawarabayashi, and S. Jegelka, "Representation learning on graphs with jumping knowledge networks," in *International Conference on Machine Learning*. PMLR, 2018, pp. 5453–5462.
- [35] M. Chen, Z. Wei, Z. Huang, B. Ding, and Y. Li, "Simple and deep graph convolutional networks," in *International Conference on Machine Learning*. PMLR, 2020, pp. 1725–1735.
- [36] G. Li, C. Xiong, A. Thabet, and B. Ghanem, "Deepergcn: All you need to train deeper gcns," *arXiv preprint arXiv:2006.07739*, 2020.
- [37] G. Bouritsas, F. Frasca, S. Zafeiriou, and M. M. Bronstein, "Improving graph neural network expressivity via subgraph isomorphism counting," *IEEE Transactions on Pattern Analysis and Machine Intelligence*, vol. 45, no. 1, pp. 657–668, 2022.
- [38] M. Yang, R. Wang, Y. Shen, H. Qi, and B. Yin, "Breaking the expression bottleneck of graph neural networks," *IEEE Transactions on Knowledge and Data Engineering*, 2022.
- [39] E. Abbe, "Community detection and stochastic block models: Recent developments," *Journal of Machine Learning Research*, vol. 18, no. 177, pp. 1–86, 2018. [Online]. Available: <http://jmlr.org/papers/v18/16-480.html>
- [40] D. P. Kingma and J. Ba, "Adam: A method for stochastic optimization," *arXiv preprint arXiv:1412.6980*, 2014.